American Mineralogist, Volume 76, pages 1319–1327, 1991

Oscillatory zonation patterns in hydrothermal grossular-andradite garnet: Nonlinear dynamics in regions of immiscibility

Bjørn Jamtveit
Department of Geology, University of Oslo, P.O. Box 1047 Blindern, N-0316 Oslo 3, Norway

Abstract

Grossular-andradite (grandite) garnet, precipitated from hydrothermal solutions associated with contact metamorphism in the Oslo rift, shows complex oscillatory chemical zonation. Immiscibility in the grandite system at $T \leq 400$ °C, $P \approx 500$ bars has been demonstrated by coexisting, unzoned isotropic and anisotropic grandite garnets in skarn zones around hydrothermal veins. A set of three first-order differential equations model the garnet zonation as a function of internal and external factors. The model simultaneously accounts for immiscibility in the grandite system, dissipation of energy during epitaxial growth of one garnet phase upon another, and external forcings such as variations in the composition of the hydrothermal fluid(s) from which the garnets precipitate. It is demonstrated how simple (periodic) external forcings may lead to very complex (nonperiodic) zonation patterns within regions of immiscibility.

Although the observed zonation profiles may have resulted from transient rather than stationary growth processes, the model indicates that stationary nonperiodic and chaotic growth dynamics may arise in the grandite system under the influence of quasi-periodic external templates.

Introduction

Quantitative descriptions of geological systems and processes have traditionally concentrated on equilibrium systems and reversible reactions. More recent research, however, has focused attention increasingly on nonequilibrium phenomena. Studies of mass transport and combined mass transport and chemical reactions have been performed within the linear range of nonequilibrium thermodynamics where the flows (or rates) of irreversible processes are linear functions of the thermodynamic forces (e.g., Fisher, 1973; Frantz and Mao, 1976, 1979; Weare et al., 1976; Lichtner, 1985). Although many geological processes are sluggish enough to keep the geological system involved close enough to equilibrium for these approaches to be appropriate, numerous processes occur outside the linear range of thermodynamics (see Ortoleva et al., 1987). Perhaps the most fascinating feature of systems far from equilibrium is their potential to create ordered patterns in space and time ("dissipative structures") through amplifications of small fluctuations in the systems (cf. Nicolis and Prigogine, 1977).

Nonlinear dynamics have been applied in models of large scale phenomena such as global geochemical cycles (cf. Lasaga, 1980) and earthquake mechanisms (Huang and Turcotte, 1990). However, in rapidly evolving fluid-rock systems, conditions far from equilibrium may exist even on scales smaller than single mineral grains. On the grain-size scale, nonlinear processes may result in complex morphological structures, such as the self-similar (fractal) silicate mineral textures described by Fowler et al. (1989) from Archaean lava flows, or in complex, intracrystalline oscillatory zonation. Oscillatory zoning of minerals occurs in a variety of geological environments, from the low-temperature regime of diagenesis (Reeder and Prosky, 1986; Reeder and Grams, 1987) to the high-temperature regime of magmatic crystallization (Bottinga et al., 1966; Sibley et al., 1976). The compositional variations occurring between the core and the rim of a mineral grain constitute a "mineral stratigraphy" that contains important information about the dynamics of the crystal growth processes.

In this paper, the complex compositional zonation pattern of naturally grown grossular-andradite (grandite) garnet is modeled using the theory of nonlinear dynamics. The model involves three first-order differential equations that simultaneously account for (1) immiscibility in the grossular-andradite binary system at the ambient temperature, (2) dissipation of energy (dampening) during epitaxial growth of one garnet on another of different composition, and (3) external factors, notably changes in the composition of the hydrothermal fluid(s) from which the garnets precipitate.

The geological environment

During the Permian continental rifting event in the Oslo region of southern Norway, massive intrusions of acidic to intermediate batholiths at shallow crustal levels caused convective fluid transport in Cambrian to Silurian metasedimentary rocks (Goldschmidt, 1911). At the Ravndalskollen locality near the eastern margin of the Oslo

0003–004X/91/0708–1319$02.00

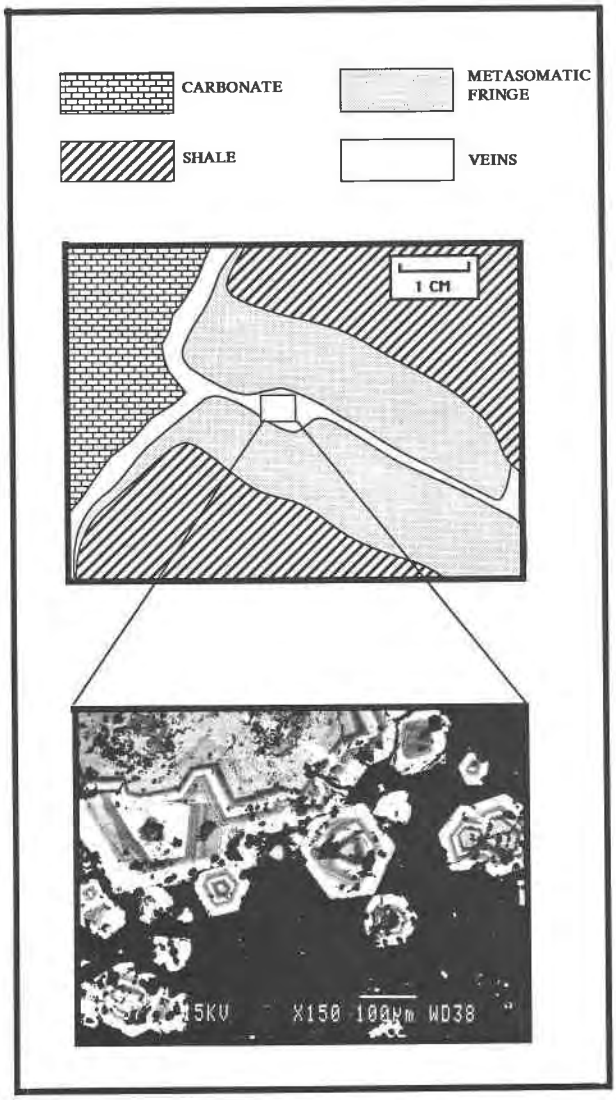

Fig. 1. Simplified sketch showing the stage III skarn and veins associated with fluid flow through brittle fractures across shale layers (**top**). The vein mineralogy consists essentially of grandite garnet, diopside, prehnite, and albite. The metasomatic fringes surrounding the fluid channels comprise a series of mineralogically distinct zones, reflecting decreasing Ca potential away from the vein contact. Note that the fringes are widest parallel to the shale foliation (striped pattern), presumably because of a relatively higher tortuosity in this direction. The backscattered electron (BSE) image (**bottom**) shows oscillatory zoned grandite garnet in a matrix of prehnite and diopside. Note the qualitatively similar zonation pattern in different garnet grains independent of the size of the crystals.

rift, intrusion of syenitic batholiths at a depth of 2–3 km caused extensive fluid flow through a layered sequence of carbonates and shales (Jamtveit et al., 1991). Infiltration of H_2O-rich fluids occurred during at least three different stages (stages I–III) in the tectonothermal history of the metasedimentary rocks in the temperature range from 400 °C (stage I) to 300–340 °C (stage III). The infiltrational events all resulted in the formation of various kinds of garnet-bearing skarns. This paper focuses mainly on the garnets from stages I and III that display the most pronounced disequilibrium features. Stage I skarn formed when aqueous fluids, originally derived from the cooling syenite, infiltrated at the shale-carbonate contact. When this fluid, initially flowing along the rock boundary surfaces, subsequently infiltrated or diffused into the carbonate layers, pink and rare dark green garnet grew at the metasomatic front together with clinopyroxene (X_{Di} = 0.35–0.75) and wollastonite. During stage III infiltration, calcite-saturated aqueous fluids occasionally entered the cm-thick shale layers through a set of crosscutting extensional veins (Fig. 1). Greenish to pink garnets precipitated within the veins together with clinopyroxene (X_{Di} = 0.60–0.90), prehnite, albite, and occasional microcline. Calcite and epidote sometimes occur as inclusions in the garnet cores. The larger garnet grains usually precipitated on the vein walls, whereas smaller grains and clinopyroxene occur in a matrix of fibrous prehnite that fills the center of the veins (Fig. 1).

Metasomatic fringes from a millimeter to a centimeter wide always parallel the fluid channels through the shales (Fig. 1). These fringes comprise a set of mineralogically different zones that reflect decreasing Ca potential away from the fluid channel (Jamtveit et al., 1991). The zone closest to the fluid channel may contain clinopyroxene, calcite, titanite, and two different populations of garnet with discretely different composition but similar morphology (although their modal abundances may be quite different, Fig. 2).

Garnet composition and structure

The garnet in stage I and III skarns frequently displays dodecahedral twinning and is commonly anisotropic (Fig. 3). Table 1 shows that the compositional variations of the garnet can be roughly described as a binary mixture of grossular ($Ca_3Al_2Si_3O_{12}$) and andradite ($Ca_3Fe_2Si_3O_{12}$). Minor components are hydrogarnet [$X_{Ca_3(Fe,Al)_2(OH)_{12}} < 0.08$], spessartine ($X_{Mn_3Al_2Si_3O_{12}} < 0.02$) and a titanium garnet end-member. (Usually the garnets contain <1 wt% TiO_2, but some rare melanitic garnets may contain up to 3 wt% TiO_2.) The grandite garnets range in composition from $X_{Gro} \approx 0.04$ to $X_{Gro} \approx 0.90$. Homogeneous garnet of a composition close to one of the end-members ($X_{Gro} < 0.2$ or $X_{Gro} > 0.8$) is isotropic or nearly isotropic, whereas garnet with intermediate composition is anisotropic. Unzoned garnet from the metasomatic fringes around brittle fractures that acted as channelways for hydrothermal fluids seem to fall in three compositionally different groups (Fig. 4). These groups are separated by compositional gaps in the intervals $0.1 < X_{Gro} < 0.35$ and $0.65 < X_{Gro} < 0.80$.

The unreversed experimental data of Huckenholz and Fehr (1982) suggest that a miscibility gap may exist within the grandite system with a critical temperature of 450–500 °C. At $T \approx 300$ °C and $P \geq 3$ kbar, this gap was

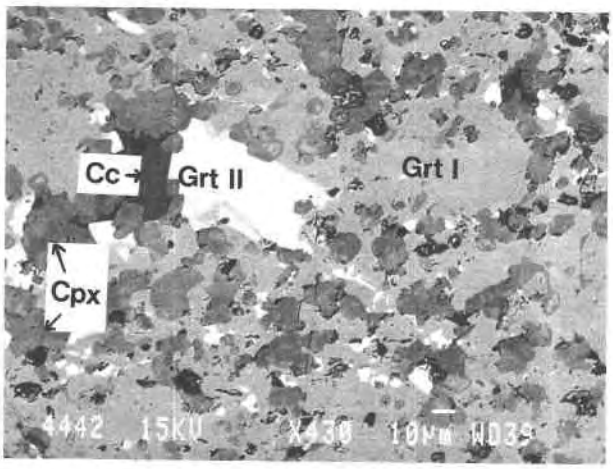

Fig. 2. BSE image showing two coexisting garnets (Grt I and Grt II), diopside (Cpx; numerous small, ≈10 μm sized, dark gray grains), and calcite (Cc; dark grain to the left of Grt II) in a metasomatic zone next to a hydrothermal vein. The garnet compositions are $X_{Gro} \approx 0.85$ (Grt I) and $X_{Gro} \approx 0.60$ (Grt II).

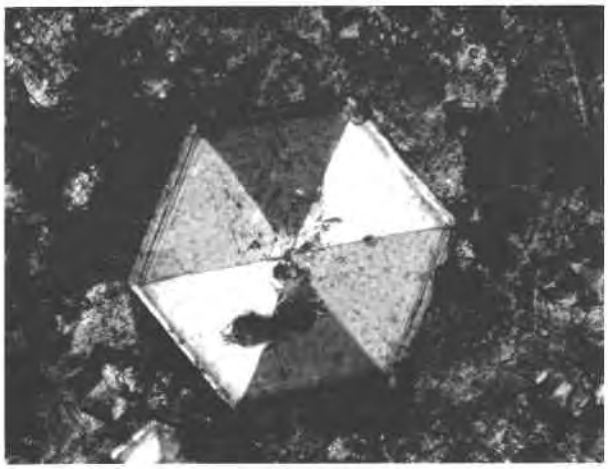

Fig. 3. Photomicrograph showing a euhedral, anisotropic grandite garnet displaying dodecahedral twinning. Plane polarized light. Field of view ca. 1 mm.

reported in the compositional interval $0.5 < X_{Gro} < 0.8$. This interval is broadly consistent with one of the compositional gaps reported above. Recently, a gap in the same compositional region has been reported from natural fluorian grandite garnets by Manning and Bird (1990). The existence of a miscibility gap within a similar region of the grandite binary is furthermore consistent with a subregular solution model for this system presented by Engi and Wersin (1987). Their solution model is based on experimental data from temperatures above 600 °C and predicts a miscibility gap in the approximate composition interval $0.65 < X_{Gro} < 0.9$ at 350 °C. Thus, the available results strongly suggest that the compositional gap found in the interval $0.65 < X_{Gro} < 0.8$ is a miscibility gap.

The status of the gap in the range $0.1 < X_{Gro} < 0.35$ is less certain. Lessing and Standish (1973) and Murad (1976) report zoned garnet with compositional discontinuities from nearly pure andradite ($X_{Gro} < 0.05$) to intermediate grandites ($X_{Gro} \approx 0.4$–0.5). However, although such discontinuities in the composition of zoned garnet would readily be explained by a miscibility gap,

Table 1. Representative analyses of unzoned matrix garnet

Sample	R891*			R887*			R8923**		
SiO_2	38.57	37.57	36.69	39.43	37.49	35.96	38.67	35.76	34.35
TiO_2	0.47	0.07	0.84	0.99	0.78	3.03	0.08	0.06	0.13
Al_2O_3	17.78	13.01	7.72	18.70	16.21	7.34	16.08	7.31	0.87
Cr_2O_3	0.01	0.00	0.00	0.02	0.00	0.00	0.00	0.00	0.00
FeO_{tot}	5.70	11.85	20.16	5.06	8.02	7.48	8.56	21.04	30.09
MnO	0.21	0.47	0.60	0.22	0.22	0.04	0.15	0.00	0.03
MgO	0.00	0.00	0.08	0.28	0.08	0.18	0.09	0.08	0.03
CaO	35.89	34.95	34.18	35.77	36.98	34.18	36.48	33.86	32.36
Total	98.82	97.92	100.27	100.47	99.78	98.21	100.11	98.11	97.85
				Normalized garnet composition (Σcations-Si = 5.000)					
Si	2.959	2.975	2.874	2.989	2.826	2.878	2.951	2.854	2.815
Ti	0.027	0.004	0.049	0.056	0.044	0.182	0.005	0.004	0.008
Al	1.608	1.214	0.713	1.671	1.440	0.693	1.447	0.688	0.084
Cr	0.000	0.000	0.000	0.001	0.000	0.000	0.000	0.000	0.000
FeIII	0.365	0.782	1.237	0.272	0.506	1.125	0.546	1.309	1.907
FeII	0.020	0.003	0.083	0.049	0.000	0.045	0.000	0.095	0.155
Mn	0.010	0.032	0.040	0.014	0.014	0.003	0.010	0.000	0.002
Mg	0.000	0.000	0.009	0.032	0.009	0.021	0.010	0.010	0.002
Ca	2.970	2.965	2.868	2.905	2.987	2.931	2.983	2.895	2.841
OH†	0.164	0.100	0.504	0.044	0.696	0.488	0.196	0.584	0.740

Note: FeO_{tot} = total Fe.
* Garnets from stage III skarn assemblages.
** Garnets from stage I skarn assemblages.
† OH calculated as 4 × (3.000 − Si).

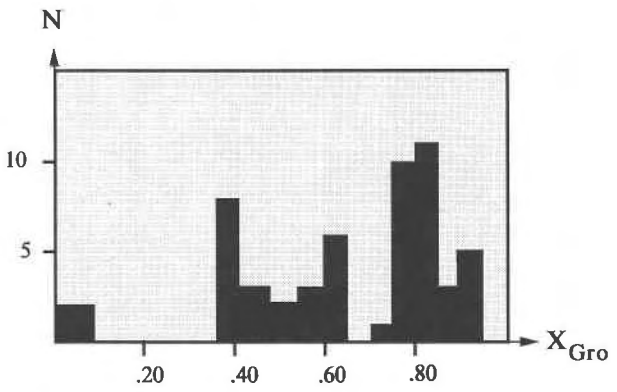

Fig. 4. Histogram showing the partitioning of garnet compositions obtained from electron microprobe (EMP) analyses of fine-grained (<100 μm), unzoned garnet from metasomatic zones close to the stage III hydrothermal veins (sample no. R891) and from andradite-rich stage I garnet (sample no. R8923). See Table 1 for representative garnet analyses. Note the apparent compositional gaps in the regions X_{Gro} = 0.10–0.35 and X_{Gro} = 0.65–0.80. Analyses are from the Cameca Camebax EMP at the Mineralogical-Geological Museum in Oslo, using natural and synthetic materials as internal standards and Cameca's Pap software for data reduction.

they may also reflect rapid fluctuations in the chemical or physical environment of the growing garnet. Thus, the observed compositional gap within the andradite-rich part of the grandite system may or may not represent a miscibility gap.

Figures 5a and 5b show the backscattered electron (BSE) image of a euhedral garnet, ca. 100 μm in diameter, that has a fairly homogeneous core surrounded by a striking oscillatory zonation, with sharp boundaries between layers of different composition. The grossular-rich parts of the garnet are nearly isotropic, whereas the andradite-richer rim is strongly anisotropic. Anisotropy in unzoned garnets is likely to result from Fe^{3+}-Al ordering on the octahedral sites of the garnet structure (Allen and Buseck, 1988; Hatch and Griffen, 1989); however, in compositionally zoned garnets, anisotropy may also result from strain arising from lattice mismatch at compositional boundaries (cf. Kitamura et al., 1986). Oscillatory zonation occurs at various scales, from the >10 μm wavelength seen in Figure 5a to the <1 μm wavelength seen in Figure 5b. This qualitative similarity on scale (self-similarity) seen in the garnet zonation pattern is strikingly similar to the geometry of some well-known fractal objects (such as Cantor-sets, cf. Mandelbrot, 1985). Even though the dynamics of natural crystal growth may occasionally produce such self-similar zonation patterns, subsequent intracrystalline diffusion would be expected to smear this fingerprint of the dynamics of the growth process unless the geological environment remains at sufficiently low temperature to inhibit solid-state diffusion even at very small scales (<1 μm). The small-scale zonation of the garnet further implies that an electron microprobe step-scan across the garnet would not record the details in the garnet composition variations since the X-ray activation volume is on the order of 5 μm^3. Therefore, the zonation profile shown in Figure 5c has been constructed from a digitized section (1500 × 400 pixels) of the BSE image in Figure 5a (see figure caption for more details). It is interesting to note that sharp compositional boundaries exist between layers with bulk composition close to X_{Gro} = 0.83–0.88 and X_{Gro} = 0.55–0.60. These compositions are within the same range as the homogeneous garnet phases in the metasomatic zones (Fig. 4), and the sharp compositional discontinuities are thus interpreted as phase boundaries.

Figure 6a shows the BSE image of a garnet from a stage I skarn grown in a matrix of calcite and diopside. A conspicuous feature of this garnet is the high density of small (<1 μm) fluid inclusion cavities commonly paralleling the growth surfaces of the garnet crystal. The concentration of these cavities shows a marked drop in the outermost grossular-rich zone (dark rim on the BSE image). The zonation profile (Fig. 6b) has been constructed in a similar way to Figure 5c and shows oscillatory behavior, initially changing between a composition close to X_{Gro} = 0.1 and X_{Gro} = 0.35. However, rimward the oscillations decrease in amplitude and are dampened toward X_{Gro} = 0.35.

A model for the zonation patterns

Most quantitative models for oscillatory zonation patterns in minerals refer to idealized periodic zonation patterns in igneous plagioclase (Haase et al., 1980; Allégre et al., 1981; Simakin, 1983). These are deterministic models based on a local system description of coupled chemical reactions and transport during the crystal growth processes; i.e., the oscillatory behavior is assumed to be the result of processes in the immediate vicinity of the growing crystal and not of an external template. The pattern is, in other words, interpreted as a result of geochemical self-organization (e.g., Nicolis and Prigogine, 1977). A local system dynamic model is supported by a commonly observed lack of intercrystal correlation of oscillatory bands in igneous plagioclase (e.g., Wiebe, 1968).

Oscillatory behavior of highly nonideal, especially low-temperature, solid solutions must depend critically on the topology of the free energy surface of the chemical system. Thus, rather than starting with a detailed quantitative description of the coupled reaction and transport processes, the present approach deals with the energetics of the garnet growth process in a more explicit and phenomenological way. This allows direct application of the formalism of classical mechanics to construct a low-order analogue model that may elucidate the dynamics of the natural grandite system. The major factors that may control the variations in the composition of the precipitating garnet are (1) the free energy potential (G) vs. composition (e.g., X_{Gro}) relations in the grandite system, (2) the extent to which the existing garnet surface favors the crystallization of a garnet of composition similar to the sur-

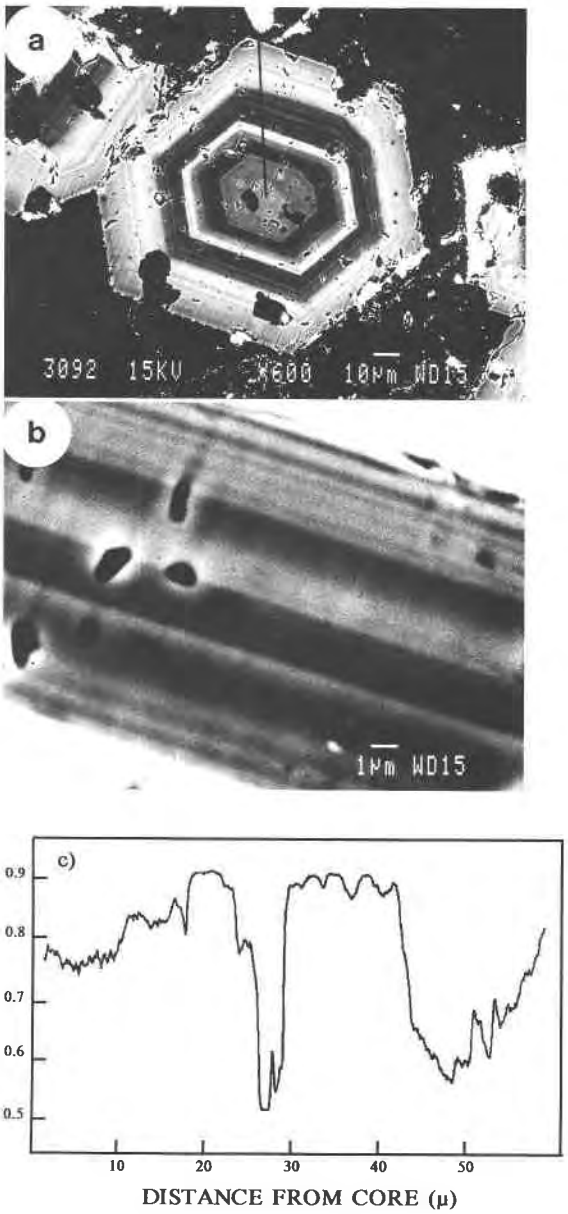

Fig. 5. (**a**) BSE image of oscillatory zoned stage III grandite garnet from a hydrothermal vein in a shale. The matrix is prehnite, and the inclusions within the garnet are diopside. Note the oscillatory zonation on two different scales. (**b**) Close-up of the widest dark band within the garnet in **a**. Note a faint oscillatory zonation with a wavelength <1 μm. (**c**) Garnet zonation profile (along the line in **a**) constructed from a digitized section (1500 $\times$ 140 pixels) of the BSE image in **a**. To reduce the noise level, the profile is based on 1500 pixels, each of which is a median value of 400 values equidistant from the rim. The ordinate variable (X_{Gro}) is taken as inversely proportional to the darkness of the BSE image. Calibration of composition from color intensity was made from 30 electron microprobe (EMP) spot analyses, each representing a volume of ≈ 5 μm^3, from the core to the rim of the garnet.

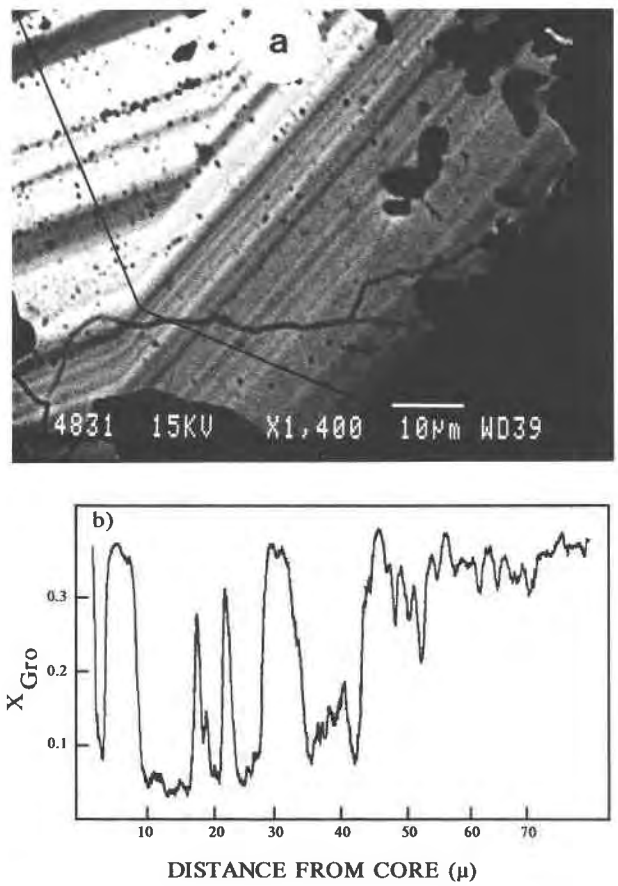

Fig. 6. (**a**) BSE image of an oscillatory zoned, andradite-rich stage I grandite garnet. This garnet contains layers with an unusual andradite-rich composition ($X_{Gro} < 0.05$), and the oscillatory behavior shows an apparent dampening rimward. Small dark spots parallel to the crystal growth surfaces are small fluid inclusion cavities. (**b**) Zonation profile (along the line in **a**) constructed from the BSE image (see caption for Fig. 5c). To reduce the noise from dark fluid inclusion voids, this profile represents the median values of 256 parallel profiles, each having 2350 pixels.

face itself, and (3) external factors such as variations in the composition of the hydrothermal fluid (especially the degree of supersaturation of the garnet components) or the P,T conditions.

The details of how the free energy potential varies with composition are largely unknown. Although useful solution models for grandite garnets exist for temperatures ≥ 600 °C (e.g., Engi and Wersin, 1987), the details of how the free energy potential of the grandite system varies with composition at temperatures relevant to this study are largely unknown. The free energy surface will probably be strongly affected by the extent of Fe^{3+}-Al disorder as a function of T in the range 300–400 °C (cf. Allen and Buseck, 1988). Therefore, the present model will be based on a simple symmetric potential that is consistent with the observation of a miscibility gap in the system of in-

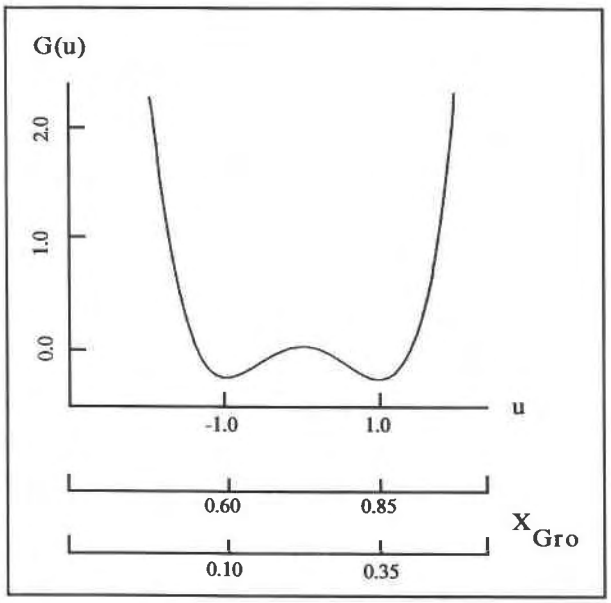

Fig. 7. Free energy vs. composition diagram used in the model presented in the text. The free energy potential (G) is symmetric and simulates the free energy potential in a region of immiscibility, here taken to be in the range X_{Gro} = 0.60–0.85 and X_{Gro} = 0.10–0.35, corresponding to the garnets in Figures 5 and 6, respectively. The potential (G) and the compositional variable (u) are appropriately scaled and dimensionless variables.

terest. The main objective of this analysis is thus not to focus on the details of the free-energy surface of the grandites but rather to investigate, in a more general way, the dynamics of crystal growth in a binary system involving regions of immiscibility.

Figure 7 shows a simple symmetric potential (G) that is consistent with the presence of miscibility gaps in the grandite system. As indicated in this figure, the following model will be presented in dimensionless form where the compositional variable (u) equals -1 and 1 at the two minima of the $G(u)$ potential. Thus, $u = -1,1$ corresponds to $X_{Gro} \approx 0.60,0.85$ for the garnet in Figure 5, implying that

$$X_{Gro} \approx 0.125u + 0.725 \tag{1}$$

or, provided that a miscibility gap also exists within the andradite-rich regions of the grandite binary, to $X_{Gro} \approx 0.05,0.35$ for the garnet in Figure 6 and thus in this case

$$X_{Gro} \approx 0.15u + 0.20. \tag{1'}$$

For simplicity, we neglect possible temperature and pressure effects and express the simple, symmetric potential $G(u)$ as

$$G(u) = \frac{u^4}{4} - \frac{u^2}{2} \tag{2}$$

so that $G(0) = 0$ and $G(\pm 1) = -0.25$ represent the two minima of the G potential. Thus in the model, the free energy of unmixing for an intermediate garnet of composition X_{Gro} = 0.725 (Eq. 1) or 0.225 (Eq. 1') corresponds to 0.25 $G(u)$ unit. In this way, the G potential is closely related to the chemical affinity (A_r) of the garnet precipitation reactions. Making an analogy with classical mechanics, the force acting on our system in this potential field is governed by the gradient of G; thus, analogous to Newton's second law, a simple model for our garnet system is provided by

$$\ddot{u}\left(=\frac{\partial^2 u}{\partial t^2}\right) = -\nabla G(u) \tag{3}$$

or

$$\ddot{u} - u + u^3 = 0. \tag{4}$$

Furthermore, epitaxial growth of a garnet of a given composition on a garnet surface of a different composition will not occur without resistance as a result of lattice mismatch (cf. Copel et al., 1989). This and other dissipation effects can be accounted for by adding a dampening term to Equation 4. The functional form of such a dampening term will depend on the detailed energetics of the crystal growth processes. However, in this low-order analogue model, we simply assume that the strain energy caused by lattice mismatch increases with the rate of change in the garnet composition. This leads to an equation of the form

$$\ddot{u} + \sigma\dot{u} - u + u^3 = 0 \tag{5}$$

where σ is a proportionality constant controlling the degree of dissipation in the system. Equation 5 describes damped oscillations attracted toward $u = \pm 1$.

The garnet composition will clearly be affected both by internal factors, such as the shape of the free energy surface of the grandite system or dissipation effects due to lattice mismatch, and by external factors (i.e., variations in the physiochemical environment of the growing garnet). Furthermore, variations in the external factors may or may not be coupled to the composition or growth rate of the garnet itself. Here we have introduced a simple potential $G(u)$ that is independent of both temperature and pressure. Thus, the only external factors affecting the garnet composition that will be considered in the following are possible variations in the composition of the hydrothermal fluid or fluids from which the garnets precipitated. Again, the functional form of the external forcing terms added to Equation 5 will be quite arbitrary and purely phenomenological.

The first situation we will consider simulates simple periodic variations in the hydrothermal fluid composition that are completely independent of the garnet growth. Adding a periodic forcing term to Equation 5 results in an equation of the form

$$\ddot{u} + \sigma\dot{u} - u + u^3 = \gamma \cos \omega t. \tag{6}$$

This equation is analogous to the Duffing equation, one of the most common examples in discussions of nonlin-

ear oscillatory systems (e.g., Guckenheimer and Holmes, 1983) and may be rewritten as an autonomous system of three first order differential equations

$$\begin{cases} \dot{u} = v \\ \dot{v} = u - u^3 - \sigma v + \gamma \cos \omega\theta \\ \dot{\theta} = 1 \end{cases} \quad (7)$$

where γ and ω control the amplitude and the frequency of the forcing. A detailed presentation of the phase-space (the space containing all possible states of the system) for this set of equations and its variations with the parameters γ, ω, and σ will not be given here. However, for a sufficiently large γ, this set of equations shows a nonperiodic (chaotic) behavior with a phase-space evolution confined to a "strange attractor" (Moon and Holmes, 1979). In the case of moderate dissipation, the chaotic behavior is not a purely transient phenomenon; it also describes the long term (stationary) evolution of the system. Large dissipation, or a small forcing term, leads to transient, nonperiodic behavior followed by damped oscillations attracted toward one of the minima of the G potential. Nonperiodic behavior may also result from quasi- or multiply periodic forcing terms.

The effects of various forcing terms are shown in Figures 8a and 8b which represent numerical solutions to Equation 6 with different values for γ and σ. In both cases (and also in Figs. 8c and 8d) the initial conditions have been chosen so that the system has sufficient energy to overcome the energy barrier at $G(0)$ for zero dissipation. This implies that the hydrothermal solution is assumed to be initially oversaturated with respect to an intermediate garnet composition corresponding to $u = 0$. Evidence for this comes from the intermediate composition of some garnet cores (e.g., Fig. 5c); however, the initial conditions are not critical to the general features of the long term evolution (zonation profile) of an externally forced dissipative system. Figures 8a and 8b reflect stationary and transient nonperiodic behavior, respectively.

The next situation we will consider is simulating the effects of external forcings from a hydrothermal fluid, the composition of which is functionally dependent on the garnet composition. Because hydrothermal solutions are very dilute with respect to mineral-forming components, the fluid in the vicinity of a growing crystal will be depleted in the crystal components unless the fluid flow through the system is very rapid. In the garnet case, this would cause changes in the affinity of the garnet precipitation reactions. Such a functional dependence between the forcing and the garnet composition reduces the variance of the system and leads to periodic behavior. Figure 8c shows the periodic zonation pattern arising from an equation that includes a forcing term that grows with time as the garnet composition $u(t)$ differs from a composition (u_B) corresponding to the bulk composition of the garnet components in the hydrothermal fluid:

$$\ddot{u} + \sigma\dot{u} - u + u^3 = -\beta \int_0^t u(t) - u_B \, dt \quad (8)$$

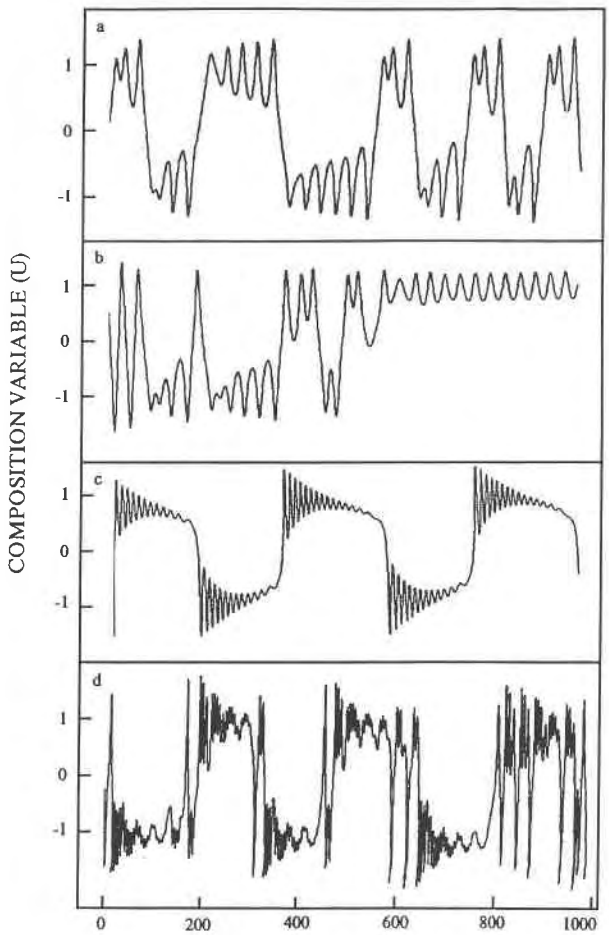

Fig. 8. Calculated zonation profiles obtained by numerically solving Equations 6–8 with various dampening parameters and forcing terms: **(a)** a solution to Equation 6 for $\sigma = 0.3$, $\gamma = 0.3$, $\omega = 1.0$; **(b)** a solution to Equation 6 for $\sigma = 0.15$, $\gamma = 0.225$, $\omega = 1.0$; **(c)** a solution to Equation 8 for $\sigma = 0.2$, $\beta = 0.08$; **(d)** a solution to a combination of Equations 6 and 8 using the forcing terms from both equations and the parameters $\sigma = 0.12$, $\gamma = 1.0$, $\omega = 0.5$, $\beta = 0.03$. Note the nonperiodic behavior of the solutions **a, b,** and **d.**

where β is a proportionality factor. This forcing term ensures that the time-integrated garnet composition, as determined from a one-dimensional zonation profile (volume effects are ignored for simplicity), equals u_B as time approaches infinity.

An example of the complexity that may arise from slightly more complex forcing terms is shown in Figure 8d where the two forcing terms of Equations 6 and 8 are added together. It is evident that making the forcing terms slightly more complex rapidly leads to exceedingly complex zonation patterns.

Comparison of the measured garnet zonation profiles and zonation patterns calculated from our simple ana-

logue model reveals several differences in the details. These arise not only from insufficient detailed knowledge of the shape of the free-energy surface, of the functional forms of dissipation effects, and of the external forcings on the natural garnet system, but also from the nonlinear nature of the processes. Even if the deterministic, mathematical model is correct, the pattern would depend heavily on the initial conditions. This is characteristic of nonlinear chaotic dynamics that have been much discussed in recent technical and popular literature on deterministic chaos. However, there are also a number of similar elements between the measured and the calculated zonation profiles. The observed profiles show a general lack of periodicity and show large changes between two compositional levels with smoother oscillations (at least if the core and rim compositions are ignored). The profile in Figure 6b is strikingly similar to the calculated profile with large dissipation and low external forcing (Fig. 8b). This zonation pattern is clearly the result of nonstationary, transient processes. This may also be the case for the profile in Figure 5c; however, the theory indicates that even stationary chaotic behavior may arise under the influence of a periodic external template, at least if the free energy potential in the model resembles the real potential in the grandite system.

Discussion

Oscillatory zonation patterns have been a well-known but poorly understood feature of grandite garnets. Earlier descriptions of similar garnets (Lessing and Standish 1973; Murad 1976) are consistent with the observations reported here. A characteristic feature of all these zonation profiles is the abrupt changes in chemistry from one intracrystal layer to another. These sharp contacts have earlier been taken as an indication of rapid crystal growth or rapid changes in the composition of the hydrothermal solution. However, the data presented above suggest that these contacts may instead represent phase boundaries. This does not, however, exclude the possibility of relatively rapid growth from a rapidly changing hydrothermal solution.

The garnet growth rate may be related to either the degree of supersaturation (kinetically controlled growth rate) or the rate of mass transport through the hydrothermal solution (transport controlled growth rate under local equilibrium conditions). In the present case, evidence for a substantial degree of supersaturation stems from the occurrence of small euhedral garnets in the center of the hydrothermal veins, which may indicate that the hydrothermal fluid was sufficiently oversaturated with respect to garnet to allow homogeneous nucleation. Furthermore, as mentioned above, the intermediate composition of some garnet cores may imply that the fluid was supersaturated with respect to an intermediate garnet composition within a region of immiscibility (i.e., a garnet with a composition close to $u = 0$ in terms of the dimensionless composition variable). An observation that may indicate changes in the garnet growth rate is the marked decrease in the density of fluid inclusions near the rim of some stage I garnets (Fig. 6b). This decrease may plausibly be explained as a decrease in the growth rate of the garnet, because a decrease in the growth rate probably would lead to a reduction of the density of imperfections on the garnet surface where minute fluid inclusions may be trapped. Stabilization of the interface between a planar crystal and a solution is well known to be favored by low growth rates (e.g., O'Hara et al., 1968). In the kinetic case, a reduction of growth rate implies a reduction in the chemical affinity of the garnet precipitation reactions, and by reference to the model presented above, the compositional oscillations would be attracted toward one of the minima of the G potential (i.e., $u = \pm 1$). This is precisely what is observed (Fig. 6b). On the other hand, if the decrease in growth rate resulted purely from less efficient supply of garnet components from the hydrothermal fluid, additional factors would have to be invoked to explain the subsequent more grossular-rich garnet phase. In short, kinetic growth-rate control automatically relates the decrease in growth rate and the dampening of the oscillations observed in Figure 6b, whereas transport control requires an additional explanation for the changes in the shape of the zonation profile.

The model presented above demonstrates how nonlinear processes may control zonation patterns in binary solid solutions with regions of immiscibility. Nonlinear behavior may arise even in the case of periodic external forcings or templates. This is a result of the local maximum on the free energy potential [at G ($\mu = 0$) in the model] and the dissipation of energy by growth of one garnet composition upon another. This analysis offers a general understanding of the underlying dynamics reflected by a nonperiodic oscillatory zonation pattern, based on a dimensionless formulation of the theory. At present, thermodynamic data are inadequate to portray accurately the free energy (G) composition (e.g., X_{Gro}) relations in grandite solutions. Future thermodynamic data may permit a more detailed dimensional analysis and simulation of garnet growth processes in naturally grown grandite garnets. However, even at this stage, the analysis allows new insight into the dynamics of a subcritical binary system away from thermodynamic equilibrium. In fact, the oscillatory zonation patterns in grandite garnet may represent an example of dissipative structures in geosystems at a scale where the local equilibrium approximation has generally been regarded as a reasonable assumption in metamorphic systems. The theory further predicts that, under certain conditions, stationary chaotic behavior (time evolution) may arise as a result of purely deterministic dynamics.

The approach used here may be applied to the analysis of the effects of external forcings on other dynamical systems of geological interest where the topology of the relevant potential surface is complex. This is commonly the case for solid solutions at low temperatures but may also apply to phase transitions in other multicomponent systems.

Acknowledgments

Discussions and critical comments by Jan Frøyland, Kurt Bucher, W.L. Griffin, P.C. Lichtner, and G. Nicolis, and technical and computational assistance by Helge Sanvei, Tor Lønnestad, Otto Milvang, Odd Trondal, and Turid Winje are gratefully acknowledged. Constructive reviews by Martin Engi and James K. Russell significantly improved an earlier version of the manuscript. Financial support was given by the Norwegian Research Council (NAVF) grants no. 440.90/043 and 440.90/003.

References cited

Allégre, C.J., Provost, A., and Jaupart, C. (1981) Oscillatory zoning: A pathological case of crystal growth. Nature, 294, 223–228.

Allen, F.M., and Buseck, P.R. (1988) XRD, FTIR, and TEM studies of optically anisotropic grossular garnets. American Mineralogist, 73, 568–584.

Bottinga, Y., Kudo, A., and Weill, D. (1966) Some observations of oscillatory zoning and crystallization of magmatic plagioclase. American Mineralogist, 51, 792–806.

Copel, M., Reuter, M.C., Kaxiras, E., and Tromp, R.M. (1989) Surfacants in epitaxial growth. Physical Review Letters, 63, 632–635.

Engi, M., and Wersin, P. (1987) Derivation and application of a solution model for calcic garnet. Schweizerische Mineralogische und Petrographische Mitteilungen, 67, 53–73.

Fisher, G.W. (1973) Nonequilibrium thermodynamics as a model for diffusion-controlled metamorphic processes. American Journal of Science, 273, 897–924.

Fowler, A.D., Standley, H.E., and Daccord, G. (1989) Disequilibrium mineral textures: Fractal and non-fractal features. Nature, 341, 134–138.

Frantz, J.D., and Mao, H.K. (1976) Bimetasomatism resulting from intergranular diffusion: I. A theoretical model for monomineralic reaction zone sequences. American Journal of Science, 276, 817–840.

——— (1979) Bimetasomatism resulting from intergranular diffusion: II. Prediction of multimineralic zone sequences. American Journal of Science, 279, 302–323.

Goldschmidt, V.M. (1911) Die Kontakmetamorphose im Kristianiagebeit. Skrifter fra det Norske Vitenskaps Akademi, Oslo, Matematisk Naturvitenskapelig Kl., 11, 405 p.

Guckenheimer, J., and Holmes, P.J. (1983) Nonlinear oscillations, dynamical systems, and bifurcations of vector fields. Springer Verlag, New York.

Haase, C.S., Chadam, J., Feinn, D., and Ortoleva, P. (1980) Oscillatory zoning in plagioclase feldspar. Science, 209, 272–274.

Hatch, D.M., and Griffen, D.T. (1989) Phase transitions in the grandite garnets. American Mineralogist, 74, 151–159.

Huang, J., and Turcotte, D.L. (1990) Evidence for chaotic fault interactions in the seismicity of the San Andreas fault and Nankai trough. Nature, 348, 234–236.

Huckenholz, H.G., and Fehr, K.T. (1982) Stability relationships of grossular + quartz + wollastonite + anorthite II. The effect of grandite-hydrograndite solid solution. Neues Jahrbuch für Mineralogie Abhandlungen, 145, 1–33.

Jamtveit, B., Bucher-Nurminen, K., and Stijfhoorn, D.E. (1991) Contact metamorphism of layered metasediments in the Oslo rift: I. Buffering, infiltration and the mechanisms of mass transport. Journal of Petrology, in press.

Kitamura, K., Iyi, N., Kimura, S., Chevrier, F., Devignes, J.M., and Le Gall, H. (1986) Growth-induced optical anisotropy of epitaxial garnet films grown on (110)-oriented substrates. Journal of Applied Physics, 60, 1486–1489.

Lasaga, A. (1980) The kinetic treatment of geochemical cycles. Geochimica et Cosmochimica Acta, 44, 815–828.

Lessing, P., and Standish, R.P. (1973) Zoned garnet from Crested Butte, Colorado. American Mineralogist, 58, 840–842.

Lichtner, P.C. (1985) Continuum model for simultaneous chemical reaction and mass transport in hydrothermal systems. Geochimica et Cosmochimica Acta, 49, 779–800.

Mandelbrot, B.B. (1985) The fractal geometry of nature, 468 p. Freeman, New York.

Manning, C.E., and Bird, D.K. (1990) Fluorian garnets from the host rocks of the Skaergaard intrusion: Implications for metamorphic fluid composition. American Mineralogist, 75, 859–873.

Moon, F.C., and Holmes, P.J. (1979) A magnetoelastic strange attractor. Journal of Sound Vibrations, 65, 285–296.

Murad, E. (1976) Zoned birefringent garnets from Thera Island, Santorini Group (Aegean Sea). Mineralogical Magazine, 40, 715–719.

Nicolis, G., and Prigogine, I. (1977) Self-organization in nonequilibrium systems, 491 p. Wiley, New York.

O'Hara, S., Tarshis, L.A., Tiller, W.A., and Hunt, J.P. (1968) Discussion of interface stability of large facets on solution grown crystals. Journal of Crystal Growth, 3-4, 555–561.

Ortoleva, P., Merino, E., Moore, C., and Chadam, J. (1987) Geochemical self-organization: Reaction transport feedbacks and modelling approach. American Journal of Science, 287, 979–1007.

Reeder, R.J., and Grams, J.C. (1987) Sector zoning in calcite cement crystals: Implications for trace element distributions in carbonates. Geochimica et Cosmochimica Acta, 51, 187–194.

Reeder, R.J., and Prosky, J.L. (1986) Compositional sector zoning in dolomite. Journal of Sedimentary Petrology, 56, 137–247.

Sibley, D.F., Vogel, T.A., Walther, B.M., and Byerly, G. (1976) The origin of oscillatory zoning in plagioclase: A diffusion and growth controlled model. American Journal of Science, 276, 275–281.

Simakin, A.G. (1983) A simple quantitative model for rhythmic zoning in crystals. Geokhimiya, 12, 1720–1729.

Weare, J.H., Stephens, J.R., and Eugster, H.P. (1976) Diffusion metasomatism and mineral reaction zones: General principles and application to feldspar alteration. American Journal of Science, 276, 767–816.

Wiebe, R. (1968) Plagioclase stratigraphy: A record of magmatic conditions and events in a granite stock. American Journal of Science, 266, 690–703.

Manuscript received April 17, 1990
Manuscript accepted March 15, 1991